



# Effect of aliovalent Si/Bi partial substitution on propagation mechanisms of cracking and dislocation in Bi-2212 crystal system

T. Turgay<sup>1</sup> · G. Yildirim<sup>2</sup>

Received: 16 December 2018 / Accepted: 28 February 2019 / Published online: 8 March 2019  
© Springer Science+Business Media, LLC, part of Springer Nature 2019

## Abstract

This comprehensive study delves into the differentiation of mechanical performance and mechanical characteristics of Bi-site Si partial substituted  $\text{Bi}_{2.1-x}\text{Si}_x\text{Sr}_{2.0}\text{Ca}_{1.1}\text{Cu}_{2.0}\text{O}_y$  superconducting ceramic materials with the assistant of Vickers microhardness measurements performed at the indentation test loads intervals 0.245 N–2.940 N. It is found that the propagations of voids, dislocations and cracks in the Bi-2212 crystal lattice accelerate dramatically because of the dramatic increment in the sizes of crack-producing omnipresent flaws, crack initiation sites, stress concentration regions, strain fields and stress raisers in the crystal matrix with enhancing the Si/Bi partial substitution level. Hence, the presence of Si inclusions in the Bi-2212 superconducting crystal structure makes the active and independent slip systems cancel immediately, and the cracks locate more rapidly into the critical propagation speed. The load required to break the material diminishes due to the reduced durable tetragonal phase. Namely, the Si inclusions favor considerably the intergranular fracture in the host crystal matrix. Besides, it is noted that the sensitivity to the applied load raises remarkably with the substitution level due to the entanglement of dislocations and cracks with each other. As for the mechanical characterization, all the materials studied exhibit the standard indentation size effect behavior (*ISE nature*) but in the reduction trend with the substitution level. All the findings are also supported by the bulk density and residual porosity parameters. The bulk density experimental results confirm the regression of elastic properties and fracture strength with the Si/Bi substitution level. At the same time, we survey the original mechanical hardness parameters at the vicinity of plateau limit regions via the Hays–Kendall (*HK*) and indentation-induced cracking (*IIC*) approaches for the first time. According to the experimental measurement results, the *IIC* model is observed to be the best theoretical model to discuss the load-independent Vickers hardness parameters of Bi-site Si partial substituted Bi-2212 ceramic compounds.

## 1 Introduction

Superconductivity was discovered on the mercury heavy metal exposed to cooling below 4.1 K (the characteristic critical transition temperature value for the mercury) by Dutch physicist Heike Kamerlingh Onnes in 1911 [1]. In essence, the superconductivity phenomenon is shortly defined in two fundamental concepts. The first concept is related to exactly zero electrical resistance under the critical transition temperature when the second one ascribes to the expulsion of magnetic flux fields at the external magnetic fields higher

than such a value of critical magnetic field value [2]. The latter phenomenon is quantum mechanically characterized by Meissner effect (no magnetic flux density in the interior region). In other words, a superconducting material expels all the applied magnetic fields (ejection of magnetic field lines from the interior region of superconducting material) during its superconducting state [3].

Beginning of the dawn of superconductivity era, many different characteristic materials such as the metals, semi-metals, chalcogens, organic, carbon, heavy fermions, alloys, rare-earth borocarbides, pyrochlore oxides, A-15 phase, ruthenocuprates, silicon-based crystal, chevrel phase and cuprate-layered perovskite superconducting compounds driving the superconductivity are discovered sequentially. Every material discovered exhibits the superior characteristics to each other. Some of them obtain somewhat higher current and magnetic field capacities whereas the others present extremely smaller power consumption and energy dissipations founded on the

✉ T. Turgay  
tahsinturgay@gmail.com

<sup>1</sup> Department of Architecture, Sakarya University,  
54187 Sakarya, Turkey

<sup>2</sup> Department of Mechanical Engineering, Abant İzzet Baysal  
University, 14280 Bolu, Turkey

losses [4–6]. Nevertheless, throughout history of superconductivity the researchers had to, of course, overcome a series of obstacles such as the misorientation grain distributions, grain boundary coupling problems, porous structure, strong anisotropic behavior, low charge carrier (electron or hole) densities, large metal–insulator phase boundary, oxygen-defect multilayered perovskite structures, formation of active and effective electron–phonon (superconductivity and transition of the isolated grains) coupling probabilities, high anisotropy, phase volume fractions, mixed valence states with a partial oxidation of  $\text{Cu}^{2+}$  and  $\text{Cu}^{3+}$ , pair wave function, hardening/softening problems of phonons, large penetration depth length or short coherence length, sensitivity against the applied magnetic field and current, vibrational mode intensities and extremely brittleness nature [7–10]. In fact, the researchers have still tried to improve the fundamental characteristic features (provided above) of superconductors so that the materials can widely be used in much more application fields as regards the electro-optic, heavy-industrial technology, engineering, metallurgical, power transmission, refrigeration, spintronics, electric power cable, medical imaging technology, future hydrogen society, sensitive process control, magnetic separation, motor, innovative energy infrastructure, magnetic energy storage and large-scale areas [11–16]. Particularly, the cuprate superconducting ceramic materials have drawn a lot of attention in the potential application areas due to their intrinsic greater engineering magnetic field and current carrying capabilities, enormously smaller power consumption and energy dissipations founded on the losses. However, the porous structure and brittleness nature are the most problematic quantities for the restriction of cuprate ceramics.

In the present study, we survey how two fundamental problems (porous structure and brittleness nature) in the Bi-2212 crystal lattice (one of cuprate ceramic inorganic compounds) vary with the partial aliovalent replacement of  $\text{Bi}^{3+}$  impurities for the  $\text{Si}^{4+}$  foreign inclusions in the crystal lattice by the assistant of Archimedes water displacement (for porosity investigations) and Vickers hardness measurements (for the mechanical performance) done at the applied test loads between 0.245 N and 2.940 N. Furthermore, the load-independent Vickers hardness parameters ( $H_v$ ) of the pure and Bi-site Si partial substituted Bi-2212 cuprate-layered perovskite superconducting samples in the plateau (saturation limit) regions are characterized by the available theoretical models regarding indentation-induced cracking and Hays–Kendall approaches.

## 2 Experimental details for pure and Bi-site Si partial replaced Bi-2212 ceramic materials

The present study is the continuation of a systematic characterization studies founded on the influences of aliovalent Si/Bi partial replacement on the dc electrical resistivity, superconducting, phase volume fraction, energy barrier formation, structural, texturing, surface morphology, flux pinning strength, vortex lattice period, bulk density, crystallinity, grain boundary coupling problem, strength coupling quality of interaction between the superconducting grains, mechanical performance, key mechanical design and mechanical characteristic properties for Bi-site Si partial substituted  $\text{Bi}_{2.1-x}\text{Si}_x\text{Sr}_{2.0}\text{Ca}_{1.1}\text{Cu}_{2.0}\text{O}_y$  superconducting compounds.

One can see the experimental procedures (experimental measurement set-ups, press load, chemical powder purity, grinding machine, stoichiometric proportion, electronic balance, etc.) and preparation conditions (standard solid-state reaction method, heating–cooling rates, calcination–sintering temperature, time and atmospheric environment) in the published paper in Refs. [17, 18]. Besides, the role of Si/Bi partial replacement on some characteristic features such as the superconducting, dc electrical resistivity, flux pinning mechanism, crystal structural, grain boundary coupling qualities are seriously provided in [17, 18]. Shortly, in the papers the experimental details are as follows.

All the powder of chemicals including the carbonates and oxides such as  $\text{Bi}_2\text{O}_3$ ,  $\text{SrCO}_3$ ,  $\text{CaCO}_3$ ,  $\text{CuO}$  and  $\text{SiO}_2$  within the high purity of about 99.99% or higher are obtained from Alfa Aesar exclusive distributor and are weighed exactly with regard to the stoichiometric ratios by using the electronic balance. The prepared chemicals are milled in a grinding machine for 9 h in the atmospheric pressure condition standards to minimize the particle sizes and especially to get much more homogeneous mixture of chemicals. Right after, the homogenous mixture is manually grounded in the agate mortar by use of the poulder for the duration of 30 min. without any solvent or solution. Thus, we achieve the desired formation of particle sizes in the mixture and now the mixture of powder is ready for the calcination process that will be conducted in the programmable furnace (Protherm Model) at 800 °C for 24 h. Both the heating and cooling rates are performed in the porcelain crucibles at 5 °C per min under the medium of air. The resultant powder of chemicals is manually regrounded for 30 min in the agate mortar and exposed to anneal (for the main heating process) at 850 °C for 36 h. The annealed chemicals are pressed into the pellets as the rectangular bars within  $15 \times 5 \times 2 \text{ mm}^3$  sizes by means of 300 MPa

load in the atmospheric pressure condition. The solid pure and Bi-site Si partial substituted  $\text{Bi}_{2.1-x}\text{Si}_x\text{Sr}_{2.0}\text{Ca}_{1.1}\text{Cu}_{2.0}\text{O}_y$  superconducting materials are thenceforward described as the pure, Si/Bi-1, Si/Bi-2, Si/Bi-3, Si/Bi-4, Si/Bi-5 and Si/Bi-6 according to the mole-to-mole ratios of  $x = 0.010, 0.030, 0.050, 0.070, 0.100$  and  $0.300$ , respectively.

On the other hand, this paper focuses sensitively on the crucial variations of mechanical performance (mechanical durability, impact resistance, stiffness, fracture strengths and flexural strengths) and mechanical characteristics founded on the standard indentation size effect (abbreviated as *ISE*) and unusual reverse indentation size effect (known as *RISE*) behavior with the aid of Vickers hardness measurements. Moreover, we determine the original mechanical hardness parameters at the vicinity of plateau (saturation) regions by using the Vickers microhardness curves via the available theoretical approaches including Hays–Kendall and indentation-induced cracking approaches. Based on the mechanical curves, the differentiation of elastic recovery mechanism, stress-induced phase transformations, reversible/irreversible deformations, stress raisers, critical propagation speeds, critical stresses, crack-producing omnipresent flaws, crack initiation sites, Griffith critical lengths, and especially propagation mechanism founded on the growth of cracks, flaws, voids and dislocations. The role of Si inclusions on the crack propagation along the intergranular regions or transgranular regions is also discussed phenomenologically.

As for the experimental procedure, all the materials are sensitively sanded to obtain far smoother surface and more regular impression shapes in the diagonal forms for the best measurement results. The materials prepared are vertically fitted into a SHIMADZU HVM-2 tester and the microhardness experiments are exerted in atmospheric pressure at the atmospheric pressure condition standards under five various applied indentation test loads changing from 0.245 N to 2.940 N for 10 s. The lengths between two impression diagonal tracks are numerically recorded by the use of calibrated microscope within the accuracy of about  $\pm 0.1 \mu\text{m}$ . All the experiments are repeated three times at different locations (to avoid work hardening and different surface effects) on the surface of materials to get much more accurate experimental results. Furthermore, the mechanical characterizations (*ISE* and *RISE* natures) of materials are determined using the variation of microhardness parameters with the impression test loads. In literature, the standard *ISE* behavior ascribes to the non-linear reduction (inverse dependence) of original microhardness values whereas the untypical *RISE* feature is related to the non-linear increment (direct dependence) with enhancing the indentation test load applied [19–21]. We also perform the bulk density measurements with the assistant of Archimedes water displacement method and calculated the degree of granularity (residual porosity) parameters for all the materials. Finally, we examine the

influence of indentation test load on the volume fraction porosity founded on the elastic modulus.

### 3 Results and discussion

In the current paper, firstly we will determine the differentiation of key design mechanical performance properties and mechanical characteristic features (*ISE* and *RISE* behavior) via the microhardness experimental measurements exerted in the indentation test loads varying from 0.245 N to 2.940 N. Then, the hardness parameters in the saturation (plateau) limit regions of Vickers microhardness curves will allow us to explore the true (load-independent) mechanical hardness parameters by using the available theoretical models as regards the Hays–Kendall and indentation-induced cracking approaches. In the third section of Results and discussion part, we examine the role of Si/Bi partial substitution in the host Bi-2212 crystal matrix on the bulk density and degree of granularity with the assistant of Archimedes water displacement method.

#### 3.1 Experimental microhardness measurement results

It is well known that there is a close relationship between the propagation mechanisms of cracks, flaws, voids and dislocations and the fundamental mechanical performances of materials. Therein, the cracks and dislocations lead to emerge the strain fields playing an important role on not only the variation of mobility and reproduction capability of new dislocations, but also the increment in the sizes of crack-producing omnipresent flaws, growth of initial cracks, crack initiation sites and stress raisers in the crystal system. During the deformation process of a material, much fraction of applied energy resulting in the deformation is dissipated as the heat energy when the remainder is internally stored. The major portion of remaining energy is used by the strain energy related to the crack and dislocation mechanism. On this basis the critical stress values, being responsible for repressing the dislocation movement and crack propagation, diminish constantly with the deformation. Accordingly, the propagations of crack and dislocation in the crystal lattice are out of control, and thus a bit less load is required to break the material (meaning the decrement in the durable tetragonal phase). In this part, we examine the change in the deformation mechanism and related evolutions with the aliovalent Si/Bi partial substitution in the crystal lattice of polycrystalline  $\text{Bi}_{2.1-x}\text{Si}_x\text{Sr}_{2.0}\text{Ca}_{1.1}\text{Cu}_{2.0}\text{O}_y$  solid materials with the assistant of microhardness experimental measurements. The Vickers hardness results measured are graphically provided in Fig. 1. According to the figure, the presence of Si foreign impurity in the crystal system augment the dislocation

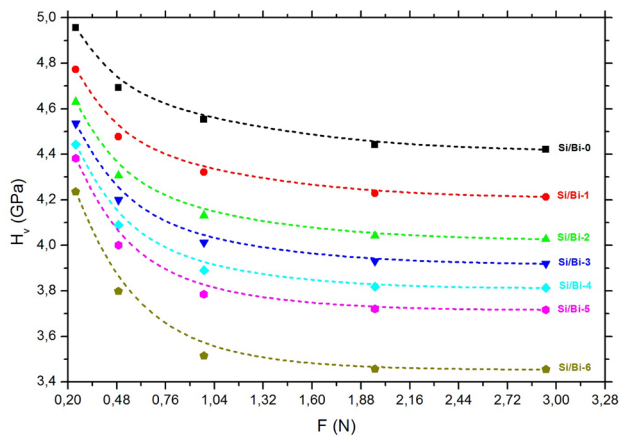


**Fig. 1** Variation of Vickers hardness parameters against applied indentation test load for un-substituted and aliovalent Si/Bi partial substituted materials

density, sizes of crack-producing omnipresent flaws and especially growth of initial cracks as a consequence of the increment in the number of dislocations, stress raisers and crack initiation sites in the crystal system. In other words, the existence of Si individuals in the crystal lattice makes the intrinsic cracks and dislocations exist new ones or enlarge remarkably. Similarly, the enhancement in the deformation mechanism is also explained that the partial aliovalent substitution of  $\text{Bi}^{3+}$  impurities for the  $\text{Si}^{4+}$  individuals in the Bi-2212 crystal lattice serves as new crack and dislocation formation sites founded on the stress concentrations such as induced permanent crystal structure problems, local structural defects, lattice strains, partial melting/voids/cracks/disorders/distortions, grain alignment distributions and grain boundary coupling problems in the crystal structure. Crack and dislocation interactions (due to the partial silicon substitution) are, of course, possible between each other and may lead to the appearance of new forces associated with the fields of growth of cracks and dislocation interactions (strain fields). Thus, new strain fields can weaken the mechanical performance of Bi-2212 superconducting crystal system.

Moreover, the dislocation motion occurs along with the specific directions or slip system (combination of the slip plane and direction) based on the crystal system. For all the superconducting crystal structures, there are the specific slip systems in which the plane has the densest atomic packing (meaning the highest planar density) and the slip direction is most closely packed with atoms (meaning the greatest linear density). Besides, the slip plane, of course, may include several slip directions. In this respect, the crystal structure of polycrystalline materials may have several slip systems with the varied possible combinations for the slip planes and slip directions, leading to strengthen the key design mechanical properties of compounds. Thus, it is not wrong to confirm

**Table 1** Vickers hardness ( $H_v$ ), elastic modulus ( $E$ ) and relative volume fraction porosity values for polycrystalline un-substituted and Bi-site Si substituted  $\text{Bi}_{2.1-x}\text{Si}_x\text{Sr}_{2.0}\text{Ca}_{1.1}\text{Cu}_{2.0}\text{O}_y$  superconducting ceramic materials

Materials	$F$ (N)	$H_v$ (GPa)	$E$ (GPa)	Relative volume fraction porosity (%)
Pure	0.245	4.956	406.211	Optimum value
	0.490	4.692	384.573	2.842
	0.980	4.553	373.180	4.370
	1.960	4.442	364.082	5.607
	2.940	4.421	362.361	5.843
	0.245	4.773	391.212	1.962
	0.490	4.478	367.033	5.204
Si/Bi-1	0.980	4.322	354.246	6.963
	1.960	4.229	346.624	8.026
	2.940	4.213	345.312	8.210
	0.245	4.630	379.491	3.521
	0.490	4.307	353.017	7.133
	0.980	4.131	338.591	9.159
	1.960	4.042	331.296	10.199
Si/Bi-2	2.940	4.027	330.067	10.376
	0.245	4.535	371.704	4.570
	0.490	4.199	344.165	8.371
	0.980	4.012	328.838	10.552
	1.960	3.931	322.199	11.513
	2.940	3.919	321.215	11.656
	0.245	4.443	364.164	5.596
Si/Bi-3	0.490	4.089	335.149	9.648
	0.980	3.89	318.838	12.003
	1.960	3.818	312.937	12.870
	2.940	3.813	312.527	12.930
	0.245	4.382	359.164	6.283
	0.490	4.001	327.936	10.682
	0.980	3.785	310.232	13.270
Si/Bi-4	1.960	3.721	304.986	14.051
	2.940	3.717	304.658	14.100
	0.245	4.235	347.115	7.957
	0.490	3.798	311.297	13.112
	0.980	3.515	288.102	16.610
	1.960	3.457	283.348	17.344
	2.940	3.455	283.184	17.369

that the mechanical duration and stiffness of polycrystalline ceramic materials with more different crystallographic orientations in the crystal structure are much higher than the single-crystal equivalents. All in all, much greater stresses applied are required for the polycrystalline materials to initiate the slip and attendant yielding as compared to the single-crystal equivalents (anticipated as the effect of geometrical constraints). In the present study, relatively few of active and independent slip systems exist for the host Bi-2212

superconducting crystal structure, and some operable slip systems are canceled by the Si dopant inserted in the crystal lattice (see Fig. 1; Table 1). The possibility of decrement in the active slip systems makes the Bi-2212 crystal matrix present the quite brittle nature. It is another probable reason for the degradation in the fundamental mechanical performances of Bi-2212 crystal structure with the partial aliovalent substitution of Bi impurities by the Si inclusions that the dopant ions change harshly the orientation of slip plane and direction within the plane, meaning the reduction in the slip capability (trend) of adjacent grains. Although the Bi-containing cuprate superconducting materials obtain some advantages due to their random crystallographic orientations of many superconducting grains (meaning the variation of slip direction between the grains), the Si/Bi partial substitution damages significantly the most favorable orientations due to the induced distortions of individual grains.

Moreover, we determine the preference of crack propagations along the intergranular regions (known as the grain boundaries) with the mechanical curves instead of the transgranular regions (or in the superconducting grains) with the increment in the Si/Bi partial substitution level (Fig. 1). Hence, the existence of Si foreign impurities in the host Bi-2212 superconducting crystal structure much more favor the intergranular fracture (weakening or embrittling the grain boundary regions). This gives a perfect representation of degrade in the crack orientation and geometry with the applied test load; consequently, the cracks reach more quickly to the critical propagation speed. Shortly, the degradation in the mechanical performances (mechanical strength, impact resistance, durability, stiffness, fracture and flexural strengths) is clearly discussed by the rapid increment in the sizes of crack-producing omnipresent flaws, growth of initial crack and dislocation motion (related to the cancel of active and independent slip systems in the Bi2212 crystal lattice).

As for the numerical values for the Vickers hardness ( $H_v$ ) parameters at the various test loads, we make the calculations with respect to the following relation (1):

$$H_v = \frac{2F \sin(\alpha/2)}{d^2} = 1.8544 \left( \frac{F}{d^2} \right) \quad (1)$$

in the equation, where  $F$  is related to the applied indentation test load (kgf),  $d$  shows the reasonable mean diagonal length (mm),  $\alpha$  is face angle of  $136^\circ$  for the indenter, and abbreviation of  $H_v$  presents the microhardness value. The constant of 1.8544 in the relation comes from the value of  $2 \sin(\alpha/2)$ . The computations are sensitively given in Table 1. It is visible from the table that the real or load-dependent Vickers hardness parameters calculated tend to decrease regularly with the Si/Bi partial substitution level. This is attributed to the fact the existence of Si inclusions in the Bi-2212 superconducting crystal matrix damages seriously the mechanical performance directly related to the mechanical strength,

impact resistance, durability, stiffness, fracture and flexural strength of polycrystalline Bi-2212 superconducting ceramic materials. Namely, the un-substituted material exhibits the Vickers hardness value of 4.956 GPa at 0.245 N whereas the  $H_v$  parameter rapidly reduces towards to the global minimum point of 4.235 GPa at the same test load. The scenario is based on the conformation that the Si inclusions embedded in the host Bi-2212 superconducting crystal lattice considerably enhance the induced permeant structural deformations, crack initiation sites, sizes of crack-producing omnipresent flaws, growth of initial cracks in the crystal system (regression of crystal structure quality as well as the interaction strength between the grains). In other words, the Si/Bi partial substitution harms strongly the most favorable orientations of some active/operable slip systems.

Moreover, it is another probable result deduced from Table 1 that all the  $H_v$  values for the Si/Bi partial substituted materials are observed to reduce remarkably with increasing the indentation test loads up to the maximum load point of 2.940 N due to the augmented strain fields, stress concentrations and stress raisers in the crystal matrix. In this regard, when the  $H_v$  values are found to be in a range of 4.956 GPa (at 0.245 N)–4.421 GPa (at 2.940 N) for the un-substituted polycrystalline material, the  $H_v$  parameter is obtained to reduce towards the global minimum value of 4.421 GPa at the constant test load of 2.940 N for the Si/Bi-6 material. This is in association with the fact that the sensitivity to the applied indentation test load tends to increase considerably with the substitution level due to the entanglement of dislocations and cracks with each other (Fig. 1). Furthermore, it is necessary to underline that generally the significant decrement (especially for the Si/Bi-5 and Si/Bi-6 samples) is present in the Vickers microhardness parameters up to the critical test load value of about 2 N, after the certain value, the Vickers parameters remain constantly due to the presence of load independent regions. According to the curves in Fig. 1, of the materials the solid Si/Bi-6 ceramic compound reaches most easily to its plateau limit value.

Lastly, all the experimental  $H_v$  curves recorded show that the un-substituted and aliovalent Si/Bi partial substituted materials exhibit the non-linear decrement in the original microhardness against the applied test loads (*ISE* feature: appearance of both the elastic and plastic deformations in the crystal structure) but in the reduction trend as the substitution level increases. Namely, the pure sample shows the strongest *ISE* characteristic behavior whereas the Si/Bi-6 superconducting material displays the minimum *ISE* feature.

### 3.2 Experimental bulk density and degree of granularity for polycrystalline un-substituted and Bi-site Si substituted $\text{Bi}_{2.1-x}\text{Si}_x\text{Sr}_{2.0}\text{Ca}_{1.1}\text{Cu}_{2.0}\text{O}_y$ superconducting ceramic materials

Determination of bulk density quantity related to the quality of crystal structural and strength connectivity between the grains in the crystal lattice plays an important role on the potential industrial, metallurgical, large scale and heavy-industrial technological application fields of ceramic materials. Similarly, the bulk density enables the scientists to survey the main characteristic behaviors regarding the dc electrical, structural, superconducting, surface morphology, energy barrier formation, flux pinning ability for the coupled vortices, vortex lattice period mechanism, mechanical performance and mechanical characterizations [22]. Besides, the degree of granularity or related residual porosity quantities are the related property of bulk density [23]. In the present work, we conduct Archimedes water displacement method to determine the effect of partial aliovalent substitution of  $\text{Bi}^{3+}$  impurities for the  $\text{Si}^{4+}$  foreign particles in the Bi-2212 crystal structure on the bulk density and related residual porosity (degree of granularity) quantities. One can encounter the numerical results for every material in Table 2 where it is seen that the Si/Bi partial substitution in the poly-crystallized Bi-2212 crystal matrix affects significantly the bulk density and degree of granularity parameters. This is attributed to the fact that the silicon foreign additives are partially substituted by the Bi-sites in the hole-induced Bi-2212 superconducting matrix.

Furthermore, the results deduced from the table show that the experimental bulk density evidences degrade gradually from  $5.97 \text{ g/cm}^3$  until the value of  $5.66 \text{ g/cm}^3$  with the increment in the Si/Bi partial substitution level up to the level of  $x=0.30$ . In this respect, the maximum value of  $5.97 \text{ g/cm}^3$  ascribes to the un-substituted compound whereas the minimum value of  $5.66 \text{ g/cm}^3$  is noticed for the bulk Si/Bi-6 superconducting material. Accordingly, the major reason

with the scenario discussed above is in correspondence to the fact that the pure sample is the densest while the Si/Bi-6 material exhibits the most porous structure. Namely, the crystal structure quality as well as the interaction strength between the grains in the Bi-2212 crystal lattice more and more degrades with increasing the Si/Bi partial substitution level. The variation of bulk density enables us to examine the role of Si inclusions in the crystal system on the relative residual porosity quantities. The degree of granularity parameters for the materials prepared in this work are calculated by the relation provided in Refs. [24, 25], where the optimum hole-induced Bi-2212 superconducting structure is received as  $6.30 \text{ g/cm}^3$  [26]. One can see all the computations performed for the un-substituted and Si/Bi partial substituted Bi-2212 superconductors in Table 2. According to the table, it is natural to confirm that the residual porosity values diminish from the minimum porosity value of 5.24% (for the pure sample) to the largest value of 10.16% (for the bulk Si/Bi-6 material). This is association with the fact that the increment in the substitution level leads to induce new permanent crystal structure problems, local structural defects, lattice strains, partial melting/voids/cracks/disorders/distortions, grain alignment distributions and grain boundary coupling problems in the crystal structure. This fact is also favored by the other parts.

Moreover, we examine the relative differentiation of granularity degrees (according to the porosity parameter of pure sample) with the silicon partial substitution level. The variations can be observed in Table 2. It is apparent from the table that the relative porosity parameter tends to increase systematically with the Si/Bi partial substitution level. The parameter between the pure and Si/Bi-1 material) is found to be about 0.845% while the percentage change in the relative degree of granularity for the value between pure and Si/Bi-6 material reaches to the global maximum point of 5.477%. This provides a pictorial representation of remarkable augmentation in the porous structure with the presence of Si foreign impurity due to the induced porosity servicing as the crack-producing omnipresent flaws. The practical consequence is that the increment in the porosity may be enough to explain why the elastic properties and fracture strength of Bi-2212 superconducting system get worse and worse with the Si/Bi substitution level.

At the same time, we investigate the effect of applied indentation test load on the volume fraction porosity appeared in the pure and Si/Bi partial substituted Bi-2212 superconducting materials by way of the following equation [27];

$$E = E_0(1 - 1.9P + 0.9P^2) \quad (2)$$

where the abbreviations of  $E_0$  and  $E$  parameters are elastic modulus values and the  $E_0$  values are inferred from the formula given below.

**Table 2** Change of bulk density, residual porosity and relative differentiation of granularity degrees with the Si/Bi substitution level for polycrystalline Bi-2212 ceramic compound

Samples	$\rho \text{ (g/cm}^3\text{)}$	$P \text{ (%)}$	$P_{\text{relative}} \text{ (%)}$
Pure	5.97	5.24	Received as optimum value
Si/Bi-1	5.92	6.03	0.845
Si/Bi-2	5.84	7.30	2.226
Si/Bi-3	5.81	7.78	2.754
Si/Bi-4	5.74	8.89	4.007
Si/Bi-5	5.70	9.52	4.737
Si/Bi-6	5.66	10.16	5.477

$$E = 81.9635H_v \quad (3)$$

Here,  $E_0$  is received as the optimum Young's modulus value under the test load of 0.2450 N when  $E$  is the abbreviation of elastic modulus parameters belonging to the solid polycrystalline  $\text{Bi}_{2.1-x}\text{Si}_x\text{Sr}_{2.0}\text{Ca}_{1.1}\text{Cu}_{2.0}\text{O}_y$  sample at any static compression test load such as 0.490 N, 0.980 N, 1.960 N and 2.940 N. In this regard, the  $E_0$  value is noted to be about 406.211 GPa and the numerical values for the volume fraction porosity parameters are gathered in Table 2. It is obvious from the table that the applied test load affects harshly the volume fraction porosity value. The parameter is obtained to be in a range of about 2.842% (at the test load of 0.490 N)–5.843% (at 2.940 N) for the pure sample. The volume fraction porosity values are also computed to be varying from 7.957% (at the test load of 0.245 N) to 17.369% (at the test load of 0.490 N). It is observed that similar to the Si/Bi partial substitution level, the volume fraction porosity values are found to depend strongly on the applied test load. Additionally, we decide which one (substitution or indentation) plays a much more important role on the volume fraction porosity parameter for the Bi-2212 crystal system by exploring the combination of Si/Bi substitution and indentation test load (Tables 1, 2). It is clear that the differentiation (pure and Si/Bi-6 material) of volume fraction porosity parameter with the substitution is observed to be about 6.283% at the test load of 0.245 N. On the other hand, the change of volume fraction porosity value (for the same materials) is demonstrated to be about 11.526% (extraction between 17.369% and 5.843) at the constant test load of 2.940 N. The major discussion deduced from the obtained result that the applied indentation test load is much more predominant role on the formation of porosity in the Si/Bi partial replaced Bi-2212 superconducting ceramic material. In more detail, both the Si/Bi substitution mechanism and particularly indentation test load applied lead to the increment in the crack initiation sites (formation of artificial cracks), stress raisers and stress amplification.

### 3.3 Mechanical modeling of real microhardness values at plateau regions

As well known that there are many theoretical approaches to examine the original microhardness features in the saturation (plateau) limit regions for the materials. Some of them are arranged as the Elastic–Plastic deformation, proportional sample resistance, Meyer's law, modified proportional sample resistance, indentation-induced cracking and Hays–Kendall approaches. Besides, the models allow to determine the mechanical characterization of materials studied. In the present work, we find all the load-independent (true) microhardness values in the plateau limit regions by using every model given above and realize that the results of only

two models (indentation-induced cracking and Hays–Kendall approaches) are found to be much closer to the original (true) microhardness values. Accordingly, we provide only their findings in the current paper.

#### 3.3.1 Survey of real Vickers hardness values with regard to Hays–Kendall Approach

The first model studied in this work is Hays–Kendall approach that provides us the attractive results for the mechanical performance and characterization of a material. The approach has widely been used in several papers to examine the key design mechanical performances of materials exhibiting the typical *ISE* feature [28–30]. In the successful model, the irreversible (plastic) deformation can appear only after a critic indentation test load, and in the equation the permanent plastic deformation is observed by the abbreviation of  $W$  where the elastic recovery disappears directly [31]. On this basis, the indentation diagonal length of indentation impression tracks is derived from the effective load value ( $F_{eff} = F - W_{HK}$ ) by the following relation:

$$F - W = A_{HK}d^2 \quad (4)$$

in the equation, the  $A_{HK}$  ascribes to the Vickers hardness constant when  $W$  is related to the applied test load. One can see the linear relation graphics between the applied test load  $F$  over the diagonal indentation length square  $d^2$  in Fig. 2. We find the Vickers hardness and impression load parameters ( $A_{HK}$  and  $W$ ) by using the extrapolation method (crossing points of axes), and all the computations are numerically tabulated in Table 3. It is apparent from the table that every  $W$  number is found to be positive values (pointing out the typical *ISE* feature) within the increment trend in a range of 0.0330–0.0447 N. This is in coincide with the fact that the *ISE* behavior decreases monotonously with the

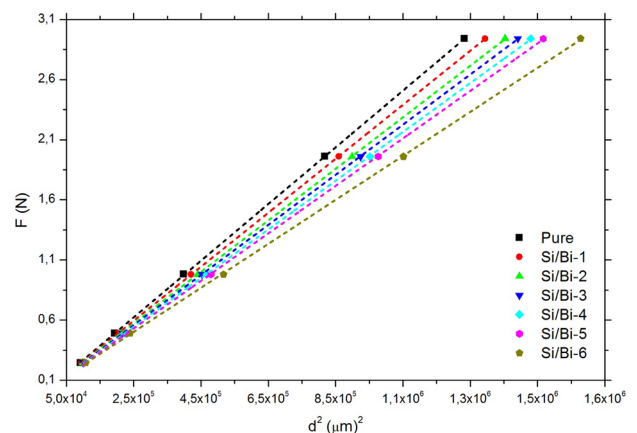


**Fig. 2** Linear plots of applied test load  $F$  over indentation diagonal length square  $d^2$  for all the superconducting materials

**Table 3** Microhardness constants based on Hays–Kendall and indentation-induced cracking models for all the materials

Samples	HK model		IIC model	
	$W \times 10^{-1}$ (N)	$A_{3HK} \times 10^{-6}$ (N/ $\mu\text{m}^2$ )	$K \times 10^{-5}$ (N $^{(3-5mA)/3}$ / $\mu\text{m}^{(2-3m)}$ )	m
Pure	0.330	2.358	115.863	−0.428
Si/Bi-1	0.332	2.245	50.125	−0.467
Si/Bi-2	0.358	2.144	11.504	−0.539
Si/Bi-3	0.362	2.085	7.583	−0.558
Si/Bi-4	0.360	2.027	6.675	−0.562
Si/Bi-5	0.374	1.975	5.095	−0.573
Si/Bi-6	0.447	1.830	2.159	−0.598

enhancement in the aliovalent Si/Bi partial substitution in the Bi-2212 crystal system. As remembered, both the elastic (reversible) and plastic (irreversible) deformations appear together in the material exhibiting the standard *ISE* feature. It is to be stressed here that the increment trend in the  $W$  number is also related to the induced permanent crystal structure problems and local structural defects in the crystal structure, being even discussed in the other parts. As for the  $A_{HK}$  parameters obtained from the  $H_v$  curves, Table 1 displays the reverse proportion between the  $A_{HK}$  constants calculated and Si substitution level. This is related to the considerable degradation in the key design mechanical performances such as the mechanical durability, impact resistance, stiffness, fracture strengths and flexural strengths due to the entanglement of dislocations and cracks with each other and particularly rapid decrement in the active and independent slip systems in the Bi-2212 superconducting crystal lattice. The findings (rapid increment in the  $W$  number and decrement in the  $A_{HK}$  constant) deduced from the Hays–Kendall approach also illustrate that the aliovalent Si/Bi partial substitution not only damages the durable tetragonal phase and critical stress, but also favors the intergranular fracture in the Bi-2212 matrix. At the same time, the model enables us to investigate the load-independent microhardness values ( $H_{HK}$ ) in the plateau limit region with the assistant of the following formula:

$$H_{HK} = 1854.4A_{HK} \quad (5)$$

One can see all the  $H_{HK}$  constants computed are inserted numerically in Table 3. It is apparent from Table 3 that the calculation results gathered according to the HK approach are observed to be a little smaller than the original Vickers hardness parameters in the saturation (plateau) limit regions (the hardness values at the vicinity of 2 N or above). Regardless, it is not wrong to claim that the calculation data are noted to be closer to the true or load-independent Vickers microhardness parameters measured. On this basis, the *HK*

theoretical approach can be received as the reliable model to discuss the original microhardness parameters in the saturation limit regions for the polycrystalline  $\text{Bi}_{2.1-x}\text{Si}_x\text{Sr}_{2.0}\text{Ca}_{1.1}\text{Cu}_{2.0}\text{O}_y$  superconducting materials.

### 3.3.2 A view to load-independent microhardness values based on indentation-induced cracking model

Researchers have appealed to the indentation-induced cracking (*IIC*) model to search the true microhardness parameters along with the plateau regions of  $H_v$  curves [32–34]. We encounter four fundamental components related the total compound resistance at the maximum indentation diagonal depth in the *IIC* model. These are sorted as;

- (i) The appearance of friction due to the indenter or specimen facet interface,
- (ii) Reversible (elastic) deformation
- (iii) Irreversible (inelastic) deformation
- (iv) Cracking of material

The first two components are directly related to the standard *ISE* feature while the last two ones generally emerge at the unusual *RISE* behavior. Therefore, the model is adequate descriptor to examine the true microhardness parameters as the permanent crystal structure problems or deformations in the crystal system increase. Maybe, the results evaluated from the theoretical approach will fit very well for the unsubstituted and aliovalent Si/Bi partial substituted materials. The original microhardness parameters are calculated from the following formula:

$$H_{IIC} = \lambda_1 K_1 (F/d^2) + K_2 (F^{5/3}/d^3) \quad (6)$$

in the equation the abbreviation of  $d$  gives the indentation size,  $\lambda_1$  denotes only a constant. When  $K_1$  presents the geometry of indenter,  $K_2$  depends on the indentation test load.  $\lambda_1$  is equal to 1 and the term of  $K_2 (F^{5/3}/d^3)$  is 0 for an ideal perfect plastic (irreversible deformation) material. Hence, the right-hand side of equation goes to  $K_1 (F/d^2)$ . Conversely,  $\lambda_1$  goes to 0 for the perfect brittle solid materials and consequently the right-hand side equals to  $K_2 (F^{5/3}/d^3)$ . Then, the equation simplifies to Eq. 7;

$$H_{IIC} = K \left( \frac{F^{5/3}}{d^3} \right)^m \quad (7)$$

Here  $K$  and  $m$  parameters show the load independent constants. One can observe the differentiation of  $\ln(H_v)$  as a function of  $\ln(F^{5/3}/d^3)$  for the pure and Bi-site Si partial substituted Bi-2212 superconducting compounds in Fig. 3. The constants of  $K$  and  $m$  extracted from the extrapolation method (crossing points of axes) are provided in Table 4. It is visible from the table that the  $m$  parameter computed



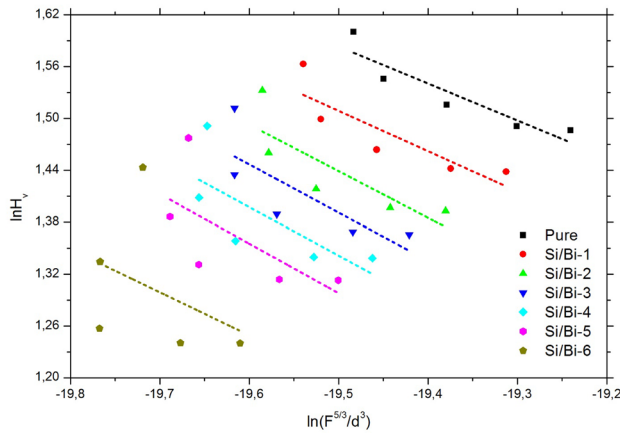


**Fig. 3** Differentiation of  $\ln H_V$  versus  $\ln(F^{5/3}/d^3)$  for all the materials prepared

**Table 4** Comparisons of original microhardness parameters of  $H_V$ ,  $H_{HK}$  and  $H_{IC}$  in the plateau limit regions

Samples	$H_{HK}$ (GPa)	$H_{IC}$ (GPa)	$H_V$ (GPa)
Pure	4.373	4.622	4.956–4.421
Si/Bi-1	4.163	4.749	4.773–4.213
Si/Bi-2	3.976	4.231	4.630–4.027
Si/Bi-3	3.866	4.129	4.535–3.919
Si/Bi-4	3.759	4.020	4.443–3.813
Si/Bi-5	3.662	3.881	4.382–3.717
Si/Bi-6	3.394	3.691	4.235–3.455

tends to diminish regularly with the increment in the Si/Bi substitution level in the Bi-2212 crystal structure. The decrement stems from the induced new permanent crystal structure problems, local structural defects, lattice strains, partial melting/voids/cracks/disorders/distortions, grain alignment distributions and grain boundary coupling problems in the solid Bi-2212 crystal system. The similar trend is observed for the  $K$  parameters. Moreover, we examine the true microhardness parameters in the saturation limit regions by comparing the experimental  $H_V$  and calculated  $H_{IC}$  values (Table 4). It is obvious that all the calculations are found to be much closer to the experimental findings in the saturation regions. In this respect, it is tempting to confirm that the  $IIC$  model is the most reliable and suitable approach to discuss the real Vickers hardness parameters of Bi-site Si partial substituted Bi-2212 ceramic compounds [19].

## 4 Conclusion

In the present work, we try to establish the crucial links between the substitution mechanism and mechanical performance for the Bi-site Si partial substituted Bi-2212 ceramic material by the use of Vickers microhardness measurements exerted at the different test loads varying from 0.245 N to 2.940 N and bulk density measurements. All the experimental measurement results show that the presence of Si inclusions in the polycrystalline Bi-2212 crystal structure leads to enhance dramatically the sizes of crack-producing omnipresent flaws, crack initiation sites, stress concentration regions, strain fields and stress raisers. Accordingly, the partial aliovalent substitution of  $\text{Bi}^{3+}$  impurities for the  $\text{Si}^{4+}$  individuals in the superconducting crystal matrix is ploughed as a strengthening method for the increase in the key design mechanical performance (mechanical durability, impact resistance, stiffness, fracture strengths and flexural strengths) due to the acceleration of dislocation and crack propagations in the crystal lattice. It is stated more succinctly that the combination of decrement in the active and independent slip systems, and the rapid accession of cracks to the critical propagation speed results in the increment of brittle nature for the Bi-2212 ceramic material. Now, the Si/Bi partial replaced Bi-2212 superconductors are much weaker and there needs much smaller energy cost to move the cracks/dislocations in the crystal structure of solid Si/Bi-6 material as compared to that of the other materials. Moreover, we examine the influence of Si/Bi partial substitution on the mechanical characteristic features. According to the experimental results, every material produced presents the standard non-linear decrement behavior in the original microhardness over the applied indentation test loads but in the reduction trend with the substitution. In this respect, it is noted that the un-substituted sample shows the strongest  $ISE$  behavior while the Si/Bi-6 material exhibits the weakest  $ISE$  feature. This is in relation to the fact that the applied load causes much more easily the entanglement of dislocations and cracks with each other in the crystal structure of Si/Bi-6 material. This fact is also confirmed by the relation between the volume fraction porosity and elastic modulus. As for the bulk density and related residual porosity parameters, the pure sample shows the maximum density value of  $5.97 \text{ g/cm}^3$  while the minimum value of  $5.66 \text{ g/cm}^3$  is obtained for the solid Si/Bi-6 material (the most porous structure). The result is based on the bulk density findings that the increment in the Si/Bi substitution level degrades significantly the crystal structure quality and interaction strength between the superconducting grains in the Bi-2212 crystal lattice. In addition, the original microhardness parameters in the saturation limit regions

are examined by the indentation-induced cracking (*IIC*) and Hays–Kendall (*HK*) models. Based on the comparison between the results, the *IIC* model is found to provide more reliable results for the load-independent Vickers hardness parameters.

## References

- H.K. Onnes, Further experiments with liquid helium. D. On the change of electrical resistance of pure metals at very low temperatures, etc. V. The disappearance of the resistance of mercury. K. Ned. Akad. Wet. Proc. **14**, 113–115 (2011)
- T. Turgay, G. Yildirim, effect of diffusion annealing temperature on crack-initiating omnipresent flaws, void/crack propagation and dislocation movements along Ni surface-layered Bi-2223 crystal structure. Sak. Univ. J. Sci. **22**, 1211–1220 (2018)
- W. Meissner, R. Ochsenfeld, Ein neuer effekt bei eintritt der supra-leitfähigkeit. Naturwissenschaften **21**, 787–788 (1933)
- J.D. Hodge, H. Muller, D.S. Applegate, Q. Huang, A resistive fault current limiter based on high temperature superconductors. Appl. Supercond. **3**, 469–482 (1995)
- S.Y. Oh, H.R. Kim, Y.H. Jeong, O.B. Hyun, C.J. Kim, Joining of Bi-2212 high-T<sub>c</sub> superconductors and metals using indium solders. Physica C **463–465**, 464–467 (2007)
- M. Chen, W. Paul, M. Lakner, L. Donzel, M. Hoidis, P. Unternaehrer, R. Weder, M. Mendik, 6.4 MVA resistive fault current limiter based on Bi-2212 superconductor. Physica C **372**, 1657–1663 (2002)
- K. Koyama, S. Kanno, S. Noguchi, Electrical, magnetic and superconducting properties of the quenched Bi<sub>2</sub>Sr<sub>2</sub>Ca<sub>1-x</sub>Nd<sub>x</sub>Cu<sub>2</sub>O<sub>8+y</sub> system. Jpn. J. Appl. Phys. **29**, L53–L56 (1990)
- A.T. Ulgen, T. Turgay, C. Terzioğlu, G. Yildirim, M. Oz, Role of Bi/Tm substitution in Bi-2212 system on crystal structure quality, pair wave function and polaronic states. J. Alloys Compd. **764**, 755–766 (2018)
- S.B. Guner, Y. Zalaoglu, T. Turgay, O. Ozyurt, A.T. Ulgen, M. Dogruer, G. Yildirim, A detailed research for determination of Bi/Ga partial substitution effect in Bi-2212 superconducting matrix on crucial characteristic features. J. Alloys Compd. **772**, 388–398 (2019)
- H. Miao, M. Meinesz, B. Czabai, J. Parrell, S. Hong, Microstructure and J<sub>c</sub> improvements in multifilamentary Bi-2212/Ag wires for high field magnet applications. AIP Conf. Proc. **986**, 423–430 (2008)
- W. Buckel, R. Kleiner, *Superconductivity: Fundamentals and Applications*, 2nd edn. (Wiley-VCH, Weinheim, 2004)
- H.H. Xu, L. Cheng, S.B. Yan, D.J. Yu, L.S. Guo, X. Yao, Recycling failed bulk YBCO superconductors using the NdBCO/YBCO/MgO film-seeded top-seeded melt growth method. J. Appl. Phys. **111**, 103910 (2012)
- K.Y. Choi, I.S. Jo, S.C. Han, Y.H. Han, T.H. Sung, M.H. Jung, G.S. Park, S.I. Lee, High and uniform critical current density for large-size YBa<sub>2</sub>Cu<sub>3</sub>O<sub>7-δ</sub> single crystals. Curr. Appl. Phys. **11**, 1020–1023 (2011)
- T.A. Coombs, A finite element model of magnetization of superconducting bulks using a solid-state flux pump. IEEE Trans. Appl. Supercond. **21**, 3581–3586 (2011)
- G. Yildirim, Determination of optimum diffusion annealing temperature for Au surface-layered Bi-2212 ceramics and dependence of transition temperatures on disorders. J. Alloys Compd. **699**, 247–255 (2017)
- F.N. Werfel, U. Floegel-Delor, R. Rothfeld, T. Riedel, B. Goebel, D. Wippich, P. Schirrmeister, Superconductor bearings, flywheels and transportation. Supercond. Sci. Technol. **25**, 014007 (2012)
- Y. Zalaoglu, T. Turgay, F. Karaboga, G. Yildirim, Changes of fundamental characteristic properties depending on Si/Bi substitution level, in *3rd International Mediterranean Science and Engineering Congress (IMSEC 2018)*, Paper ID: 451t, pp. 1704–1708
- Y. Zalaoglu, T. Turgay, G. Yildirim, A detailed analysis founded on powder X-ray diffraction for (Bi<sub>2.1-x</sub>Si<sub>x</sub>)Sr<sub>2.0</sub>Ca<sub>1.1</sub>Cu<sub>2.0</sub>O<sub>y</sub>, in *3rd International Mediterranean Science and Engineering Congress (IMSEC 2018)*, Paper ID: 452t, pp. 1149–1154
- K. Sangwal, On the reverse indentation size effect and microhardness measurement of solids. Mater. Chem. Phys. **63**, 145–152 (2000)
- R. Awad, A.I. Abou-Aly, M. Kamal, M. Anas, Mechanical properties of (Cu<sub>0.5</sub>Tl<sub>0.5</sub>)-1223 substituted by Pr. J. Supercond. Nov. Magn. **24**, 1947–1956 (2011)
- A.A. Elmustafa, D.S. Stone, Nanoindentation and the indentation size effect: kinetics of deformation and strain gradient plasticity. J. Mech. Phys. Solid. **5**, 357–381 (2003)
- N.K. Saritekin, M. Pakdil, E. Bekiroglu, G. Yildirim, Examination of effective nucleation centers for flux pinning of vortices and optimum diffusion annealing temperature for Au-diffusion-doped Bi-2212 polycrystalline compound. J. Alloys Compd. **688**, 637–646 (2016)
- W. Abdeen, S. Marahba, R. Awad, A.I. Abou Aly, I.H. Ibrahim, M. Matar, Electrical and mechanical properties of (Bi, Pb)-2223 substituted by holmium. J. Adv. Ceram. **5**, 54–69 (2016)
- C.J. Poole, H.A. Farach, R. Creswick, *Superconductivity* (Academic Press, San Diego, 1995)
- R.R. Reddy, M. Murakami, S. Tanaka, P.V. Reddy, Elastic behavior of a Y-Ba-Cu-O sample prepared by the MPMG method. Physica C **257**, 137–142 (1996)
- K. Kocabas, M. Ciftcioglu, The effect of Sb substitution of Cu in Bi<sub>1.7</sub>Pb<sub>0.3</sub>Sr<sub>2</sub>Ca<sub>2</sub>Cu<sub>3-x</sub>Sb<sub>x</sub>O<sub>y</sub> superconductors. Phys. Status Solidi A **177**, 539–545 (2000)
- W.D. Callister Jr., D.G. Rethwisch, *Materials Science and Engineering: An Introduction*, 9th edn. (Wiley, New York, 2013)
- M. Dogruer, C. Terzioğlu, G. Yildirim, M. Pakdil, Y. Zalaoglu, Decrement of crack propagation in bulk Bi-2223 superconducting ceramics with Sn-diffusion annealing temperature. J. Mater. Sci. Mater. Electron. **26**, 6013–6019 (2015)
- Y. Zalaoglu, B. Akkurt, M. Oz, G. Yildirim, Transgranular region preference of crack propagation along Bi-2212 crystal structure due to Au nanoparticle diffusion and modeling of new systems. J. Mater. Sci. Mater. Electron. **28**, 12839–12850 (2017)
- N.K. Saritekin, H. Bilge, M.F. Kahraman, Y. Zalaoglu, M. Pakdil, M. Dogruer, G. Yildirim, M. Oz, Improvement of mechanical characteristics and performances with Ni diffusion mechanism throughout Bi-2223 superconducting matrix. AIP Conf. Proc. **1722**, 140007 (2016)
- C. Hays, E.G. Kendall, An analysis of Knoop microhardness. Metallurgy **6**, 275–282 (1973)
- M. Dogruer, O. Gorur, F. Karaboga, G. Yildirim, C. Terzioğlu, Zr diffusion coefficient and activation energy calculations based on EDXRF measurement and evaluation of mechanical characteristics of YBa<sub>2</sub>Cu<sub>3</sub>O<sub>7-x</sub> bulk superconducting ceramics diffused with Zr nanoparticles. Powder Technol. **246**, 553–560 (2013)
- B. Akkurt, G. Yildirim, Change of mechanical performance and characterization with replacement of Ca by Gd nanoparticles in Bi-2212 system and suppression of durable tetragonal phase by Gd. J. Mater. Sci. Mater. Electron. **27**, 13034–13043 (2016)
- H. Li, R.C. Bradt, The effect of indentation-induced cracking on the apparent microhardness. J. Mater. Sci. **31**, 1065–1070 (1996)

**Publisher's Note** Springer Nature remains neutral with regard to jurisdictional claims in published maps and institutional affiliations.